Efficient strategy for the occasionally proportional feedback method in controlling chaos

Tsung-Hsun Yang*
Institute of Electro-Optical Engineering, National Chiao-Tung University, Hsinchu 30010, Taiwan

Shyh-Feng Chen and Yih-Shun Gou
Institute of Electrophysics, National Chiao-Tung University, Hsinchu 30010, Taiwan

(Received 15 September 1998)

In this work, the generic mechanism of the occasionally proportional feedback (OPF) technique in controlling chaos has been explored extensively. Except for stabilizing the unstable states that are embedded in the chaotic attractors, the OPF method is also found to generate a great number of new states during the control processes. The forms and characteristics of these new states have been addressed. Moreover, we clarify the roles of the parameters in the OPF method and this clarification leads to a practical and systematic approach in adjusting the parameters for control. To demonstrate the validity, an analogous electronic circuit of the resistively shunted Josephson junction oscillator is employed in addition to a numerical illustration of the logistic mapping. [S1063-651X(99)15805-7]

PACS number(s): 05.45.Gg

I. INTRODUCTION

Since Ott, Grebogi, and Yorke (OGY) suggested a general method for stabilizing the unstable periodic orbits embedded within chaotic attractors in 1990 [1], a number of researchers have already demonstrated that chaos can be useful in a variety of fields [2–9]. The OGY algorithm is based on targeting the stable manifold of a particular unstable orbit by introducing a controlled perturbation to a system parameter. This general way to control chaos has promised great success in applications. Under such inspiration, more and more applications are designed based on the chaotic regime for its versatility and flexibility. However, the OGY control needs a complicated calculation in the dynamical controlling processes as a whole. It has to calculate the stable and the unstable eigenvalues and eigenvectors of the chosen fixed point on the Poincaré section for their respective steps throughout the execution of control. Practically, how to *effectively, exactly, and insistently* target the states in accordance with one's wishes becomes the most important and current subject for the study of the use of chaos.

Based on the idea of the OGY method, Peng, Petrov, and Showalter subsequently proposed an occasional proportional feedback (OPF) method, which can simplify the computation substantially [2]. Hunt further implemented the OPF method in an electronic circuit for controlling the chaos of a diode resonator [3] and Roy *et al.* also succeeded in taming chaos in a laser system via the OPF technique [5,6]. Indeed, because of very little dependence on systems and because there is no need for any complicated computation, the OPF technique has the potential to be employed in a wide range of applications. Nevertheless, the generic mechanism of OPF is not known completely so far. As a result, during the operation of the OPF method, people need to pursue the proper ranges of the control parameters to achieve the goal of controlling chaos. In addition whether or not the *deduced* states under the OPF are the unstable states embedded in the *original* chaotic attractor remains to be addressed. Recently, Galias *et al.* have described some theoretical results concerning the choice of control parameters and the possibilities of successful OPF control [10]. They concluded that better control results could be obtained provided that the unstable eigenvector of the target is parallel to the coordinate that is used for computing the control signal. Inaba and Nitanai discussed the number of unstable periodic orbits (UPO's) that can be stabilized via the OPF method in the voltage pulse generator [11]. To some extent, Ogorzalek modified Hunt's OPF controller, which obviates the need for an external synchronizing signal [12]. In the meantime, Tsubone and Saiton also derived some theoretical analysis in a piecewise linear circuit, such that the function of the OPF method can be guaranteed [13]. However, to find the embedded UPO's, there remains no systematic method in adjusting the control parameters of the OPF method [12]. Therefore, the subject concerning how to definitely and systematically explore the relation between the control parameters in the OPF technique and the final controlled states of the systems would be of theoretical and practical interest.

In this paper, the subject of how to systematically retrieve the embedded UPO's in the OPF control will be studied extensively. To establish the control applicability of the OPF method, the influence of each control parameter will be explored in detail. It then turns out that a key clue for systematically adjusting the parameters in the OPF method could be extracted. Section II, therein, will outline the essential idea of the OPF method. Then the selection of the control parameters of the OPF method will be illustrated and this brings out an efficient algorithm of the OPF control. In addition, to verify the analytical results and the systematic control steps, the application to the logistic map will be demonstrated in the numeric calculations. Also, in Sec. III, the resistively shunted Josephson junction (RSJ) oscillator [14–17] with external periodic driving will be also employed to demonstrate the validity of our algorithm for the OPF control. All of the

*Present address: Nonlinear Science Group, Department of Physics, National Cheng-Kung University, Tainan 70101, Taiwan.

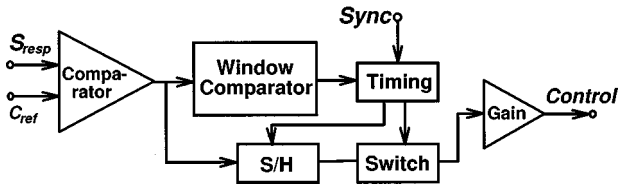

FIG. 1. Block diagram of the OPF control method.

emphasis in this section will be placed on an analogous electronic simulator as a practical demonstration. Finally, the summary and conclusion are given in Sec. IV.

II. THE OPF METHOD

The operations of the OPF control method will be described here briefly. Figure 1 shows the content of the OPF method. There are three essential parameters in the OPF control: the reference (C_{ref}), the window width (C_w), and the gain value (C_g). From the left-hand side of Fig. 1, the system response S_{resp} is compared with the reference C_{ref}. The difference is fed into the ''window comparator'' and the ''S/H'' blocks. The S/H block is a sample-and-hold unit to store the different desired values. Here, C_w defines the width of the window comparator to allow the control performed. Also, the clock ''sync'' is introduced to set up the working time in the ''timing'' block. If the difference between S_{resp} and C_{ref} is less than the window width C_w, in accordance with the clock sync, the timing block will trigger the S/H block to sample the different value, and to hold this value for later. At the same time, the timing block will also close the ''switch'' such that the held value in the S/H block can be amplified by the gain C_g in the ''gain'' block. Then, the amplified value is feedback to perturb the chosen system parameter.

Whenever the difference is larger than the window width C_w in accordance with the clock sync, the timing block will open the switch such that the control signal will not operate on the system. In this case, it means that the system response S_{resp} is away from C_{ref}. In practice, due to the characteristic ''ergodic'' feature of the chaotic states, sooner or later, the system response S_{resp} will come close to the level of C_{ref} again as time goes on. After a few cycles of operation, the chaotic response of the system will be tamed into a regular wave form.

A. The Reference C_{ref}

To explore the generic mechanism of the OPF method, let us consider the control parameter C_{ref} in the OPF method first, which gives the position of the window center for the control operation. It is worthwhile to note that only the discrete responses of the system need to be considered, and the time intervals are defined by the sync signals. This is because the OPF control only changes its amount of feedback in *discrete* time. Let the sequence of the Y_n's be the sampling of S_{resp} at the time defined by the sync. That is, the Poincaré section of S_{resp}. In this section, the fixed point is denoted as Y_F^*. The control operation is performed only when the system response Y_n is away from C_{ref} within the allowable range of the window width C_w. We note that C_{ref} relates to the desired target Y_F^*. Obviously, when C_{ref} is close to Y_F^*, the system could stay almost unperturbed as the control had achieved. At that time, the control signal will eventually be eventually close to zero.

However, the control signal may not be infinitesimal for a different setting of C_{ref}. Thus, the final controlled state in the Poincaré section may deviate away the desired target Y_F^*. In such a case, the system will be perturbed a little. Let us take the case of the period-1 state as an illustration. The fine evaluation can be understood as follows. At the nth step of the control, the system parameter, say F, will be perturbed as

$$\Delta F_n \equiv F_{n+1} - F_n = \alpha C_g (Y_n - C_{ref}), \tag{1}$$

where α is a proportional constant that is dependent on the process of the modulation of F and independent of the OPF control. Meanwhile, the unstable fixed point Y_F^* will also be perturbed to $Y_{F_n}^*$ corresponding to the variation of F at the nth step of the control. $Y_{F_n}^*$ can be linearly approximated as

$$Y_{F_n}^* \approx Y_F^* + \frac{\partial Y}{\partial F}\Delta F_n = Y_F^* + \alpha C_g (Y_n - C_{ref})\frac{\partial Y}{\partial F}. \tag{2}$$

As a consequence, the first return map function of Y_n around $Y_{F_n}^*$ could be approached in a linear approximation around Y_F^* as

$$\begin{aligned} Y_{n+1} = M(Y_n) &\simeq Y_{F_n}^* + m(Y_n - Y_{F_n}^*) \\ &= mY_n + (1-m)\left[Y_F^* + \alpha C_g (Y_n - C_{ref})\frac{\partial Y}{\partial F}\right], \end{aligned} \tag{3}$$

where m is the slope of the return map at Y_F^* and the change on m is negligible. From Eq. (3), the period-1 fixed point Y_c^* follows $Y_{n+1} = Y_n = Y_c^*$ and

$$Y_c^* = Y_F^* \frac{1 - \alpha C_g \dfrac{\partial Y}{\partial F}\left[\dfrac{C_{ref}}{Y_F^*}\right]}{1 - \alpha C_g \dfrac{\partial Y}{\partial F}}. \tag{4}$$

Thus, as C_{ref} is set close to Y_F^*, Y_c^* will be close to Y_F^*. Otherwise, Y_c^* will be away from Y_F^*, and as a result, ΔF is not negligible. This means

$$\Delta F = \alpha C_g (Y_c^* - C_{ref}) = \frac{\alpha C_g}{1 - \alpha C_g \dfrac{\partial Y}{\partial F}}(Y_F^* - C_{ref}). \tag{5}$$

Now one can figure out that most of the controlled states generated by the OPF control will be new when the feedback control is not negligible. In such a way, when ΔF is large enough, the status of the system is shifted and could possibly be switched out of the chaotic region. Under the circumstance, the linear approximation analysis for Y_c^* will not work. Nevertheless, the OPF can turn the chaotic states of the system into the simple motions of Y_c^* in a wide range of C_{ref}. But, different C_{ref} results in different final states created by the OPF control.

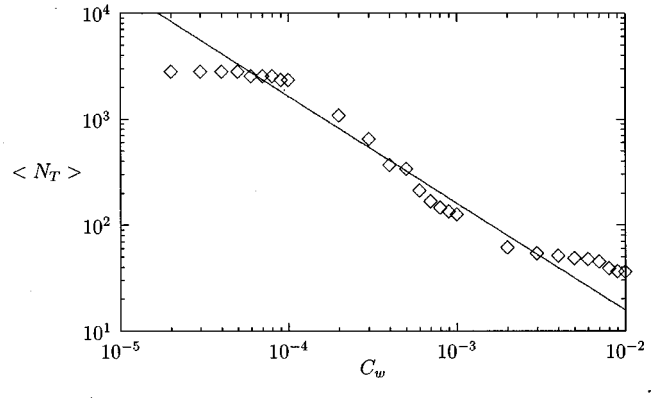

FIG. 2. Relation between the average transient iterations $\langle N_T \rangle$ and the window width C_w for the OPF control on the logistic map. The $\diamond$ symbols denote the data that are averaged over 250 random initials for each C_w, and the solid line is $C_w^{-1.010}$. Here, the parameter F of the logistic map is 0.92.

B. The window width C_w

Next, the influence of the window width C_w is considered. In fact, the value of the control parameter C_w will determine how far Y_c^* could be away from Y_F^*, since C_w is a maximum difference between Y_n and C_{ref}. Accordingly, the larger C_w is, the more allowed controlled states are. That is, for larger (smaller) C_w, there will be a wider (narrower) range of C_{ref} to achieve the control. Naturally, it should be satisfied for the controlling process that Y_c^* is located within the window centered at C_{ref} with width C_w. The condition can be written as

$$|Y_c^* - C_{ref}| \leqslant C_w . \tag{6}$$

From Eq. (4), the lower limit of C_w for the corresponding C_{ref}, thus, is found to be

$$\varepsilon \left| \frac{Y_F^*}{1 - \alpha C_g \dfrac{\partial Y}{\partial F}} \right| \leqslant C_w , \tag{7}$$

where ε is the relative error between C_{ref} and Y_F^* and defined as $|Y_F^* - C_{ref}|/|Y_F^*|$. Equation (7) is useful for practical applications. Because it is very difficult to set C_{ref} exactly equal to Y_F^*, there always exists a nontrivial least value of C_w to achieve the control. The less the precision is, therefore, a larger C_w will be required.

On the other hand, C_w is related to the transient time required for a successful control. When C_w is small, the OPF control will need a longer transient time, since it will take a few tries to reenter the region around the level set by C_{ref} and C_w to reoperate the control. Take the logistic map

$$Y_{n+1} = 4FY_n(1 - Y_n) \tag{8}$$

as an example, where F is a constant defined between [0,1]. When the target is aimed at the unstable period-1 state ($Y_F^* = 1 - 1/F$) for the arbitrary case, say $F = 0.92$, the average times of the transient iteration $\langle N_T \rangle$ for various C_w are shown in Fig.2. The values of $\langle N_T \rangle$ are averaged over 250 random initials of Y_n for each C_w. Obviously, the less C_w is, the longer the transient time will be. Moreover, $\langle N_T \rangle$ is found in the form of $C_w^{-\gamma}$. Here, $\gamma \approx -1.010$ for the case of $F = 0.92$. Unfortunately, setting C_w as large as possible cannot guarantee the success of a fast and correct control. In fact, if C_w is too large, a large amount of feedback will occur to the control signals such that the dynamical behavior that represents the whole system consists of the *target system* and the *OPF control unit*, and is no more limited only to the target system. As a result, the final dynamics often will be out of the original design.

Nevertheless, the control results should not be sensitive to C_w in some situations. As long as the regular motion is achieved, the value of C_w will not influence the final controlled states.

C. The Gain value C_g

The control parameter C_g determines the amount of the feedback from the OPF control to the system. In practical applications, to know how to adjust C_g is important. If an effective C_g is known, a great effort can be saved in control. Let us explore its influence.

For a simple presentation, the reference C_{ref} is set to the same level of Y_F^*. Similarly, the iteration of Y_n is given in Eq. (3). As a result, the deviation for each step follows:

$$\Delta Y_{n+1} \equiv Y_{n+1} - Y_F^* = \left[m + (1-m)\alpha C_g \frac{\partial Y}{\partial F} \right] \Delta Y_n . \tag{9}$$

If Y_n converges to Y_F^*, it must be $|\Delta Y_{n+1}/\Delta Y_n| < 1$ as n becomes large enough. Consequently, Eq. (9) can further be rewritten as

$$\left| m + (1-m)\alpha C_g \frac{\partial Y}{\partial F} \right| < 1. \tag{10}$$

Therefore,

$$\left(\alpha \frac{\partial Y}{\partial F} \right)^{-1} < C_g < -\frac{1+m}{1-m} \left(\alpha \frac{\partial Y}{\partial F} \right)^{-1} \quad \text{if } (1-m)\frac{\partial Y}{\partial F} < 0$$

or

$$-\frac{1+m}{1-m} \left(\alpha \frac{\partial Y}{\partial F} \right)^{-1} < C_g < \left(\alpha \frac{\partial Y}{\partial F} \right)^{-1} \quad \text{if } (1-m)\frac{\partial Y}{\partial F} \geqslant 0. \tag{11}$$

This inequality provides the range of effective C_g for successful control.

D. Efficient Strategy of Control

According to the analysis above, in what follows, the steps for efficiently employing the OPF control in applications are proposed.

(1) Learn the dynamics of the system through the return map without the OPF control.

(a) Locate one desired fixed point on the return map.

(b) Evaluate the slope m of the mapping function of the return map at the chosen fixed point.

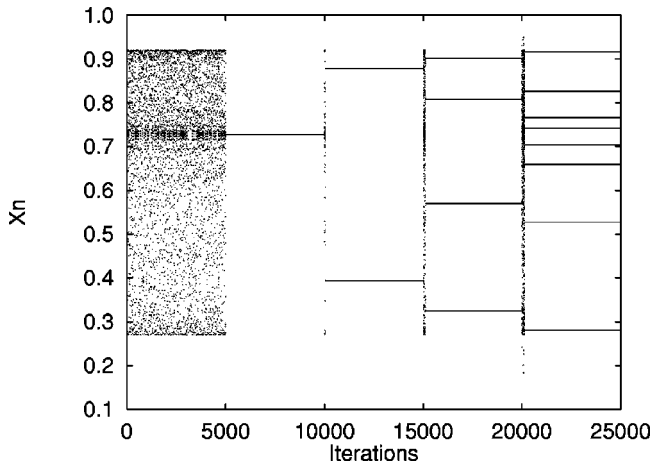

FIG. 3. OPF control results of the logistic map according to our control algorithm, where $r=0.92$. The OPF control is turned on at the 5000th iteration to the target period-1 state and changes its setting every 5000 period iterations to target the period-2, period-4, and period-8 states, respectively. All of the parameters in the control process are listed in Table I.

(c) Evaluate the gradient vector $\partial Y/\partial F$ of the chosen fixed point under the variation of the accessible parameter of the system.

(2) Apply the OPF control on the system.

(d) Set up the control reference C_{ref} at the same level as the located fixed point.

(e) Adjust the control gain C_g within the limits described by the inequality equation (11).

(f) Set up the control width C_w, starting from a small value that is greater than the lower limit in the inequality equation (7).

(g) If the control fails, go back and change C_g to another value and adjust C_w a little larger. Repeat the previous steps (e) and (f) again until the control achieved. Practically, most of cases need only one trial.

To show the validity, numerically, the logistic map [Eq. (8)] is employed to tame the chaotic states under the OPF control according to the control algorithm above. In Fig. 3, it illustrates the results of the OPF control according to our control algorithm. From the start to the 5000th iteration is the free running of the logistic map only. It is a chaotic motion. Then, the OPF control is turned on at the 5000th iteration to target the period-1 state and all three control parameters of the OPF control are changed for the different desired states ($p-2$, $p-4$, and $p-8$) every 5000 periods in sequence. All of the parameters in the control process are listed in Table I. After the control is turned on, each desired state is soon to be achieved. In this demonstration, it shows that our control algorithm can really provide a good guidepost for effectively choosing the control parameters of the OPF method. It saves a great deal of effort of finding out the proper setting of the OPF control. At least our control algorithm has improved the efficiency of employing the OPF control on the logistic map.

To be further shown below, the OPF control method is robust and easy to implement in the practical applications. With the controlling scheme above, the desired states can be achieved fast and effectively. Next, as a real-model demonstration of validity, the control algorithm shown above will be applied to the RSJ oscillator.

III. APPLICATION TO THE RSJ OSCILLATOR

For the nonlinear RSJ oscillating system with an external driving force, the equation of motion follows:

$$\ddot{x}+\kappa\dot{x}+\sin x=F\sin\omega t, \tag{12}$$

where κ denotes the damping constant, F and ω represent the amplitude and the frequency of the external periodic driving force, respectively. For the external driven RSJ oscillator, it can be utilized to describe the equation of motion of the phase difference across the Josephson junction under the microwave illumination. It can also be visualized as the dynamic motion of the swept angle of the pendulum [14,18,19], the charge density wave [19], parametric amplifiers [20,21], etc. Thus, the achievement of the control of chaos on the RSJ oscillator will provide a good reference for a wide range of practical applications. Here, instead of a direct numerical simulation, the RSJ oscillating system is constructed in analogous electronic circuits [22].

Without the loss of generality, the value of κ is chosen as 0.1. A phase diagram of the RSJ oscillator is shown in Fig. 4. Mainly, the route to chaos is the Feigenbaum period-doubling route. Meanwhile, the window of the period-3 state is observed within the chaotic regime. Fig. 5 shows the bifurcation diagram of Y_n with F as the varying parameter. It shows that the route to chaos is a Feigenbaum period-doubling cascade and a reverse cascade. As expected, the results observed through the electronic simulator are in good agreement with the previous numerical reports [23].

As a typical presentation, we take the RSJ oscillator around the region centered at the point of $\omega=0.68$, $F=2.20$, and $\kappa=1.0$. Let us follow the recipe proposed in the

TABLE I. Control parameters for different targets in the logistic map.

Iterations	Period	C_w	C_{ref}	C_g	Estimation for C_g	Lower limit of C_w
$0-5000$						
$5000-10000$	1	0.001	0.7283	$+2.00$	$+0.8590\sim+3.3856$	0.000244
$10000-15000$	2	0.001	0.3935	-1.00	$-1.4061\sim-0.5156$	0.000058
$15000-20000$	4	0.001	0.5702	$+0.70$	$+0.5697\sim+0.9008$	0.000448
$20000-25000$	8	0.002	0.6597	$+0.52$	$+0.4975\sim+0.5672$	0.001202

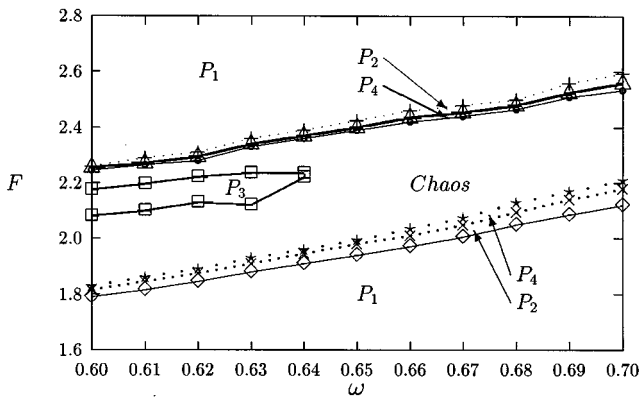

FIG. 4. Phase diagram of the RSJ model with $\kappa=1.0$. The region marked as P_n denotes the solutions with period-n states. The chaotic states are observed in the region marked ''chaos.'' This diagram is generated based on the observation of our electronic circuit.

last section. Figure 6 shows the typical return map of Y_n. To avoid the discontinuity, due to the 2π displacement operations at $x=\pm\pi$, Y_n is defined as the voltages of $\dot{x}$ sampled every time interval of $2\pi/\omega$. It is well known that the intersections of the first return map curve and the 45° line are the locations of the period-1 fixed points of the system. Since the tangent slope of the map function at the intersection is smaller than -1, this fixed point is unstable. Similarly, those period-n unstable fixed points can be detected on the nth order return map.

To check the influence of the control parameters, C_{ref} and C_w are first scanned without any specific choice. In Fig. 7, the typical result is shown — mainly, C_{ref} is continuously scanned from -1.3 to -0.8 for $C_w=0.1$, 0.3, and 0.5, respectively. The regular states can be established as C_{ref} is scanned. The occurrence of the controlled states with period-1 or period-2 fixed points are very common, while high periods of states can also be achieved correspondingly. Consequently, one can expect that the OPF control method will nicely control chaos on the RSJ oscillator system, provided that one can properly adjust the parameters. As a matter of fact, these easily obtained low-period states are good enough for the general purpose of controlling chaos in the practical applications [24,25].

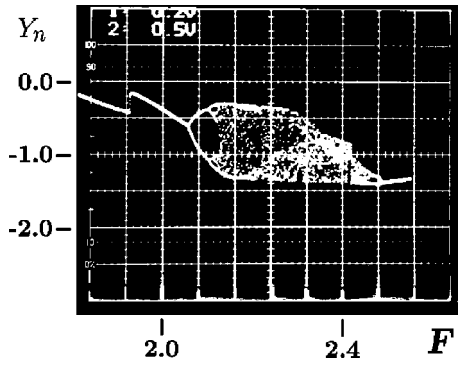

FIG. 5. Bifurcation diagram of the RSJ oscillator caused by a variation of F from 2.0 to 2.5, where $\omega=0.68$ and $\kappa=1.0$.

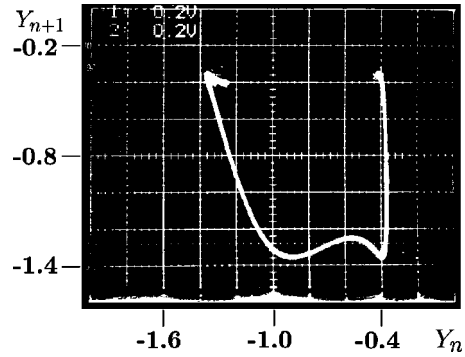

FIG. 6. First return map of the RSJ oscillator at $\omega=0.68$, $F=2.22$, and $\kappa=1.0$.

It is noted that most of the controlled states generated by the OPF control are new. For example, the RSJ oscillator without control could have only a finite number of period-1 UPO's, and these UPO's are discrete. However, with the

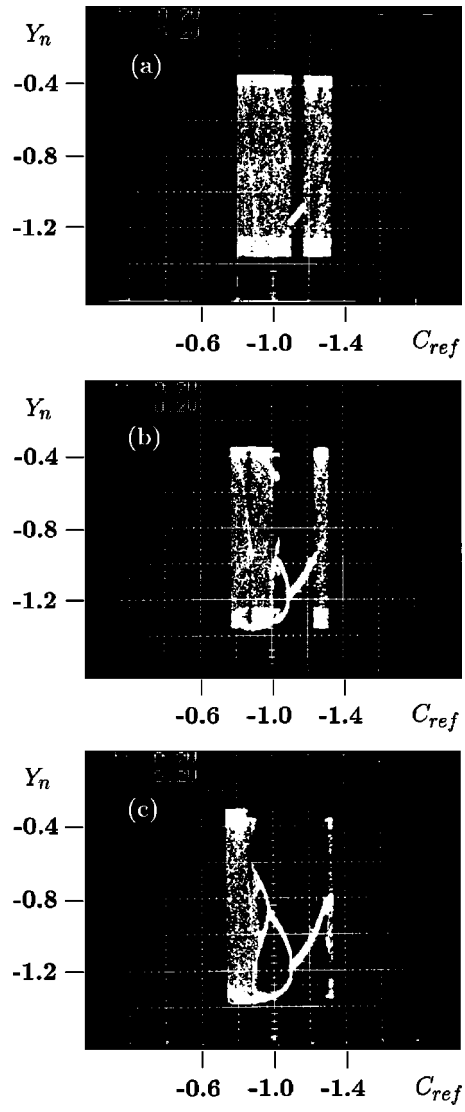

FIG. 7. Bifurcation diagram of the RSJ oscillator where C_{ref} is varied from -1.3 to -0.8, and C_w is fixed at a specific value for (a) $C_w=0.1$, (b) $C_w=0.3$, and (c) $C_w=0.5$. The rest of the parameters are $C_g=0.5$, $\omega=0.68$, $F=2.22$, and $\kappa=1.0$.

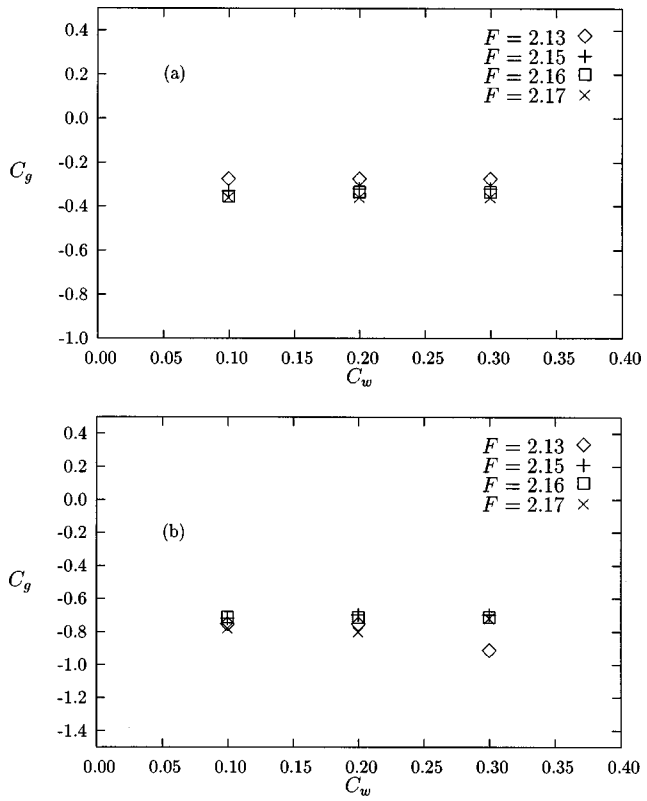

FIG. 8. Effective C_g range to C_w of the period-1 case for various F at $\kappa = 1.0$ and $\omega = 0.68$. (a) is the upper limit and (b) is the lower limit of C_g.

OPF control, a continuous band of period-1 orbits have been found by adjusting C_{ref} only (as shown in Fig. 7). Therefore, these new generated states will not simply obey the dynamics of the RSJ oscillator, but the whole dynamics, which consists of the RSJ oscillator and the OPF control. Moreover, as C_w increased (from 0.1 to 0.5, as shown in Fig. 7), the width of the range of C_{ref}, for achieving control in periodic motions, gets wider and wider. This verifies what we addressed above: the larger C_w is, the more controlled states can be found.

Next, the effective range of C_g is checked by varying C_w. The effective range of C_g for various bias F and different values of C_w in the period-1 case is shown in Fig. 8. One can see that the effective range of C_g for the desired controlled states is independent of the values of C_w. Thus, one can see that the controlled states are not sensitive to C_w as the control has been achieved.

As we have derived above, the effective range of the gain value C_g follows the inequality equation (11). We presented the comparison between the analytic result and the data from the analogous electronic circuits in Fig. (9). The good fitness between the analysis and the observation strongly supports our analysis and the control algorithm we proposed.

IV. SUMMARY AND CONCLUSION

In this work, we have explored the generic mechanism of the OPF technique in detail. We have provided a systematic approach to the OPF control. An electronic

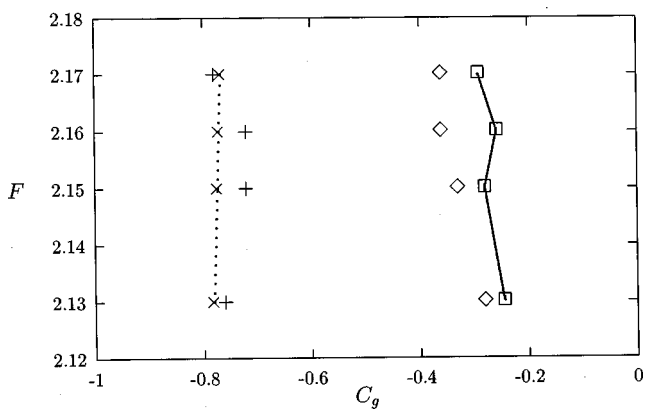

FIG. 9. Comparison between the theoretical results and the experimental data of the effective range of C_g for various F and C_w at $\kappa = 1.0$ and $\omega = 0.68$ in the case of the period-1 state. The $\times$ and $\square$ symbols denote the lower and the upper limits from the theoretical data, respectively. Symbols $+$ and $\diamond$ denote the lower and the upper limits of the experimental data.

demonstration, based on the RSJ model, has succeeded in showing the validity of the control algorithm. The OPF method is robust in taming the chaotic states of the system into the desired regular forms. As a matter of fact, in addition to extracting out the unstable states embedded in the chaotic states, the OPF method could also generate a great number of new states. The form of new states has been addressed and determined in the way of linear approximation. Here, it might be worth noting that, as to the achievement of generating new states, the OPF technique, in some sense, is similar to that of the periodic impulsive method [26]. However, its contents are out of the scope of this work.

It is worthwhile to summarize the influence of the control parameters C_w, C_{ref}, and C_g in the OPF control. The reference parameter C_{ref} indicates the level of the final target. In the meantime, the C_{ref} could cause the final controlled state to be away from the original unstable orbits. On the other hand, the window width C_w is found to be insensitive to the final control states. However, before the control is achieved, a larger C_w will reduce the transient time for the system to the target, and this also increases the chance of the occurrence of new states. As to the gain value C_g, the effective range has been derived. We noted that the effective range of C_g is independent of C_w, which fits our simulation results. As we have demonstrated, a systematic procedure for employing the OPF method can be established based on the adjustment of these three parameters, and this should be helpful in employing the OPF control for application.

ACKNOWLEDGMENTS

T. H. Yang thanks Professor J.-L. Chern for the useful comments. This work was partially supported by the National Science Councils, Taiwan, under Contract No. NSC87-2112-M-009-017.

[1] E. Ott, C. Grebogi, and J. A. Yorke, Phys. Rev. Lett. **64**, 1196 (1990).
[2] B. Peng, V. Petrov, and K. Showalter, J. Phys. Chem. **95**, 4957 (1991); V. Petrov, B. Peng, and K. Showalter, J. Chem. Phys. **96**, 7506 (1992).
[3] E. R. Hunt, Phys. Rev. Lett. **67**, 1953 (1991).
[4] W. L. Ditto, S. N. Rauseo, and M. L. Spano, Phys. Rev. Lett. **65**, 3211 (1990).
[5] R. Roy, T. W. Murphy, T. D. Maier, Z. Gills, and E. R. Hunt, Phys. Rev. Lett. **68**, 1259 (1992).
[6] Z. Gills, C. Iwata, R. Roy, I. B. Schwartz, and I. Triandaf, Phys. Rev. Lett. **69**, 3169 (1992).
[7] S. Hayes, C. Grebogi, and E. Ott, Phys. Rev. Lett. **70**, 3031 (1993).
[8] Y. C. Lai and C. Grebogi, Phys. Rev. E **47**, 2357 (1993).
[9] A. Garfinkel, M. L. Spano, W. L. Ditto, and J. N. Weiss, Science **257**, 1230 (1992).
[10] Z. Galias, C. A. Murphy, M. P. Kennedy, and M. J. Ogorzalek, Proc. ISCAS' **96**, 120 (1996).
[11] N. Inaba and T. Nitanai, IEEE Trans. Circuits Syst., I: Fundam. Theory Appl. **45**, 473 (1998).
[12] M. J. Ogorzalek, Chaos Solitons Fractals **9**, 295 (1998).
[13] T. Tsubone and T. Saito, IEEE Trans. Circuits Syst., I: Fundam. Theory Appl. **45**, 172 (1998).
[14] D. E. McCumber, J. Appl. Phys. **39**, 3113 (1968).
[15] W. C. Stewart, Appl. Phys. Lett. **12**, 277 (1968).
[16] R. L. Kautz, J. Appl. Phys. **52**, 6241 (1981).
[17] R. L. Kautz and R. Monaco, J. Appl. Phys. **57**, 875 (1985).
[18] A. H. MacDonald and M. Plischke, Phys. Rev. B **27**, 201 (1983).
[19] R. L. Kautz, IEEE Trans. Magn. **19**, 465 (1983).
[20] M. T. Levinsen, R. P. Chiao, M. F. Feldman, and B. A. Tucker, Appl. Phys. Lett. **31**, 776 (1976).
[21] R. L. Peterson and D. G. MacDonald, IEEE Trans. Magn. **13**, 887 (1987).
[22] S. F. Chen, M. S. thesis, Institute of Electrophysics, National Chiao-Tung University, Hsinchu, Taiwan, 1997 (in Chinese).
[23] T. H. Yang, C. S. Wang, J. C. Huang, and Y. S. Gou, Phys. Rev. E **51**, 5279 (1995), and references therein.
[24] B. R. Hunt and E. Ott, Phys. Rev. Lett. **76**, 2254 (1996); Phys. Rev. E **54**, 328 (1996).
[25] S. M. Zoldi and H. S. Greenside, Phys. Rev. Lett. **80**, 1790 (1998); B. R. Hunt and E. Ott, *ibid.*. **80**, 1791 (1998).
[26] Z. Liu and S. Chen, Phys. Rev. E **56**, 168 (1997); Z. Liu and S. Chen, Phys. Lett. A **232**, 55 (1997).